

# Transition to the ultimate regime in a stochastic model for thermal convection with internal sources

Marten Klein<sup>1\*</sup> · Heiko Schmidt<sup>1</sup> · Alan R. Kerstein<sup>2</sup>

<sup>1</sup>Numerical Fluid and Gas Dynamics, Brandenburg University of Technology (BTU), Cottbus, Germany

\*Contact: marten.klein@b-tu.de

<sup>2</sup>Consultant, Stochastic Science, Danville, CA, USA

## Introduction

- **Heat transport** in a layer of fluid heated from below (Rayleigh–Bénard system) is mathematically similar to **angular momentum transport** in a layer of fluid between rotating cylinders (Taylor–Couette system) (see e.g. [1]).
- **Internal sources** can destabilize the flow due to radiative heating [2, 3], internal wave breaking [4], or intermittently unstable boundary layers [5].
- In **turbulent thermal convection** a chaotic flow is driven by buoyancy forces due to an unstable temperature stratification. This type of flow is considered here and encountered in numerous applications that range from technical to atmospheric and astrophysical scales (see e.g. [6]).

## Main objectives

- Investigation of **scaling regimes** of the **heat transfer** in radiatively driven thermal convection.
- **Modeling** using a numerical tool applicable throughout the **relevant parameter space**.
- Capture **wall-normal (vertical) transport** on **all relevant scales** of the flow by utilizing the **one-dimensional turbulence** model [7].

## Model formulation

The **ODT model** aims to **resolve all relevant scales** of a turbulent flow along a notional line-of-sight ('ODT line'). Flow variables are resolved along this line on a dynamically adaptive grid [8]. Instantaneous flow profiles are evolved by **deterministic diffusion** along the ODT domain, and a **stochastic process** that models the effects of turbulent advection, pressure fluctuations, and buoyancy forces that are aligned with the ODT domain ( $z$  coordinate) [7, 9, 10].

- **ODT governing equations** for the Cartesian velocity components  $u_i$  and the temperature  $T$  are

$$\frac{\partial u_i}{\partial t} + \mathcal{E}_i(\alpha) = \nu \frac{\partial^2 u_i}{\partial z^2}, \quad \frac{\partial T}{\partial t} + \mathcal{E}_T = \kappa \frac{\partial^2 T}{\partial z^2} + \frac{Q_{\text{tot}}}{\rho_0 c_p},$$

where  $\nu$  is the kinematic viscosity,  $\rho_0$  the reference mass density,  $c_p$  the specific heat capacity at constant pressure,  $\kappa$  the thermal diffusivity, and  $Q_{\text{tot}}$  the heat sources and sinks.

- **Stochastic terms**  $\mathcal{E}_i$  and  $\mathcal{E}_T$  represent the effects of discrete turbulent **eddy events** in which the **triplet map** models the turnover of a notional turbulent eddy (Fig. 1).
- The turbulent **eddy rate**  $\tau^{-1}(\lambda, z_0; t)$  of a size- $\lambda$  eddy event at location  $z_0$  at time  $t$  depends on the **total available eddy specific energy** for the momentary flow state. The eddy rate reads [9, 10]

$$\tau^{-1} = C \sqrt{2\lambda^{-2} (E_{\text{kin}} - E_{\text{pot}} - Z E_{\text{vp}})},$$

where  $E_{\text{kin}}$  and  $E_{\text{pot}}$  denote the eddy specific kinetic and potential energy, respectively, and  $E_{\text{vp}}$  is a viscous penalty energy to suppress eddy events below a viscous length scale [7].

- **Fixed ODT model parameters**  $C = 60$ ,  $Z = 220$ , and  $\alpha = 2/3$  are used here. Definitions are identical to [10] but the calibration was performed for Rayleigh–Bénard convection with  $Pr \lesssim 1$  [11].

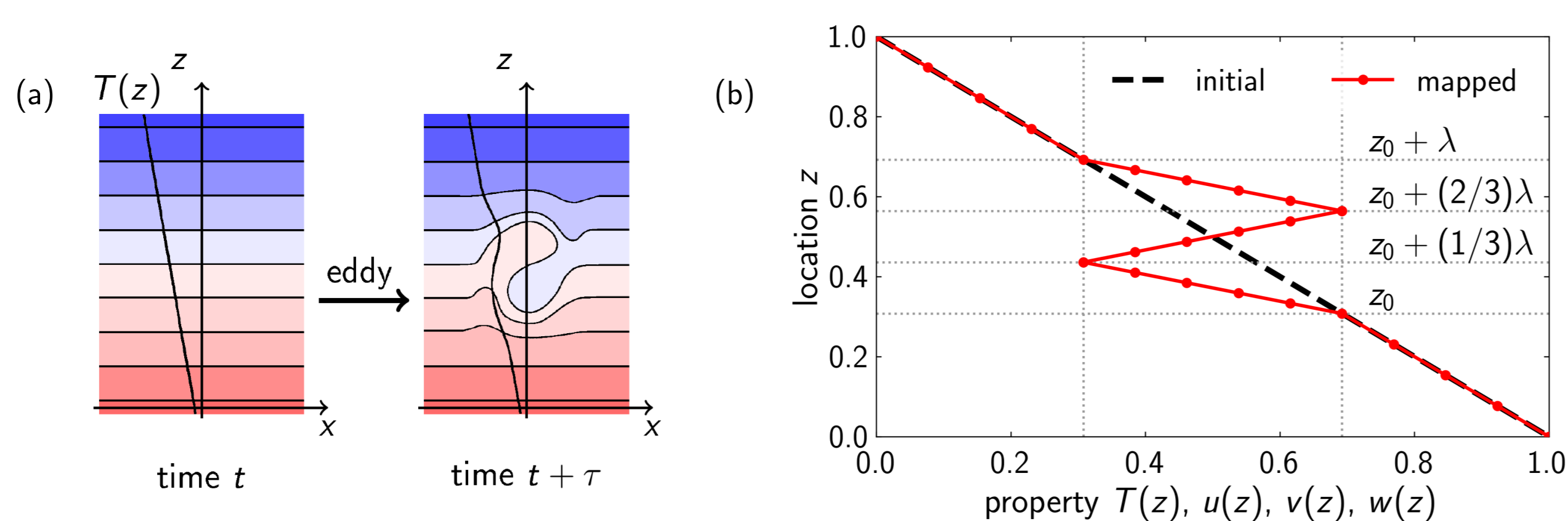


Figure 1: (a) Schematic of an eddy turnover. (b) Triplet map for an eddy event that covers the interval  $0.33 \leq z/H \leq 0.67$ .

## Flow configuration and model application

- **Layer of fluid** of height  $H$  for which wall-normal transport is resolved by a vertical ODT line (Fig. 2)
- Uniform **constant gravity**  $g = -g e_z$
- **Oberbeck–Boussinesq fluid**: linear equation of state,  $\rho(T) = \rho_0 [1 - \beta(T - T_0)]$ , where  $\beta$  is the thermal expansion coefficient, and subscript 0 denotes reference values
- **Smooth adiabatic no-slip wall** at bottom  $z = 0$  and top  $z = H$
- **Heat sources/sinks**:  $Q_{\text{tot}} = Q(z) - \langle Q \rangle_z$ , where  $Q(z) = (P/\ell) \exp(-z/\ell)$  is the local heating rate,  $-\langle Q \rangle_z$  the spatial mean cooling rate,  $\ell$  a prescribed length scale, and  $P$  the power influx [2, 3].
- The flow is characterized by the **Prandtl**, **Rayleigh**, and **Nusselt number**,

$$Pr = \frac{\nu}{\kappa}, \quad Ra = \frac{g \beta \langle \Delta T \rangle H^3}{\nu \kappa}, \quad Nu = \frac{PH}{\rho_0 c_p \kappa \langle \Delta T \rangle},$$

where  $\Delta T = T|_{z=0} - T|_{z=H/2}$  is a convenient definition of a **wall-bulk temperature difference** with temporal average  $\langle \Delta T \rangle$  [2, 3].

- The **flux-based Rayleigh number**  $Ra_0 = Ra Nu$  of the forcing is independent of  $\langle \Delta T \rangle$ .

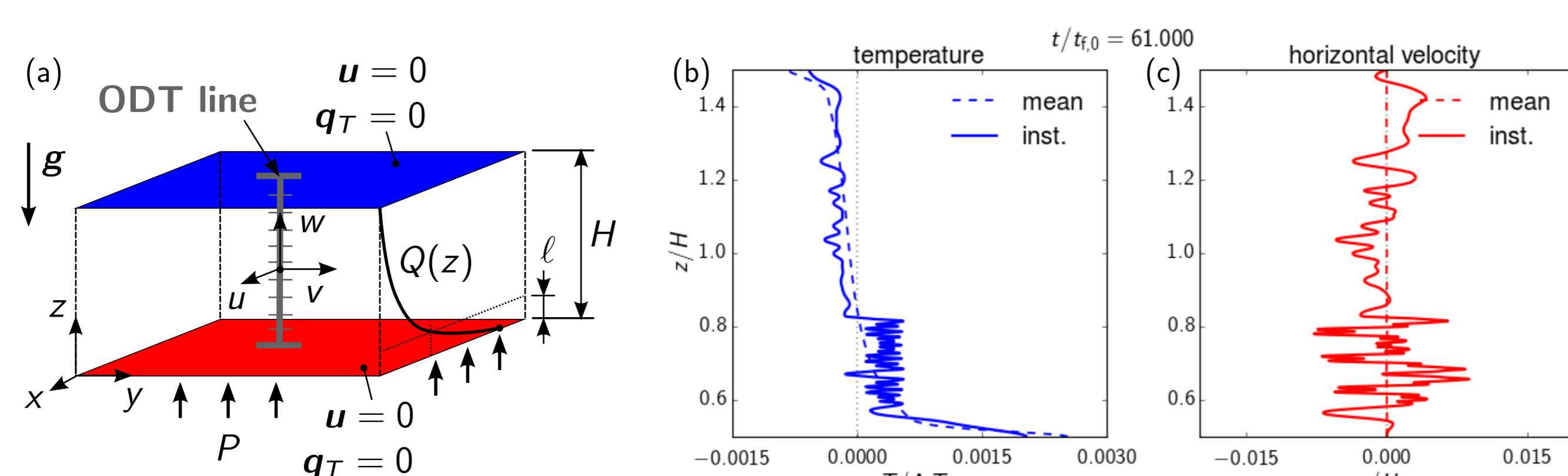


Figure 2: (a) Sketch of the set-up. The fluid is heated by the profile  $Q(z)$  with total power influx  $P$  analogous to [2]. (b) Vertical profiles of the instantaneous and mean temperature,  $T$  and  $\langle T \rangle$ , respectively. (c) Vertical profiles of the instantaneous and (vanishing) mean horizontal velocity component,  $u$  and  $\langle u \rangle$ , respectively. Control parameters are  $Pr = 1$ ,  $Ra_0 = Ra Nu = 10^{10}$ , and  $\ell/H = 0.096$ . Reference scales are given by the flux temperature difference  $\Delta T_0 = PH/(\rho_0 c_p \kappa)$ , the flux free-fall velocity  $U_{f,0} = \sqrt{g \beta \Delta T_0 H}$  and time  $t_{f,0} = H/U_{f,0}$ .

## Turbulent scaling regimes of the heat transfer

Grossmann & Lohse [12] showed that effective scalings of the heat transfer result from **bulk and boundary-layer contributions**. In the current configuration the **normalized absorption length**  $\ell/H$  is prescribed and acts a **control parameter** for the thermal boundary layer.

- **Fig. 3(a)** shows **multiple scalings** of the heat transfer in terms of

$$Nu \sim Ra^p (\ell/H)^q \quad \text{for fixed } Pr = 1.$$

Reference experimental results [2] (open symbols) are shown together with ODT simulation results (filled symbols) that exhibit good **qualitative and quantitative agreement**. Dashed and solid black lines give the classical  $p = 1/3$  [13] and 'ultimate'  $p = 0.55$  [2] scaling, respectively.

- **Fig. 3(b)** shows the **ODT extrapolation** for **rescaled data**  $Nu/Nu_X$  vs.  $Ra/Ra_X$ , where the subscript 'X' indicates a notional transition point. Following [3], we solve for the intersection of the classical [13] ( $p = 1/3, q = 0$ ) and 'ultimate' [2] ( $p \approx 0.55, q = 1$ ) scaling which yields

$$Nu_X \sim Ra_X^{1/3} \sim (\ell/H) Ra_X^{0.55}.$$

This transformation **collapses the ODT and reference data** equally well.

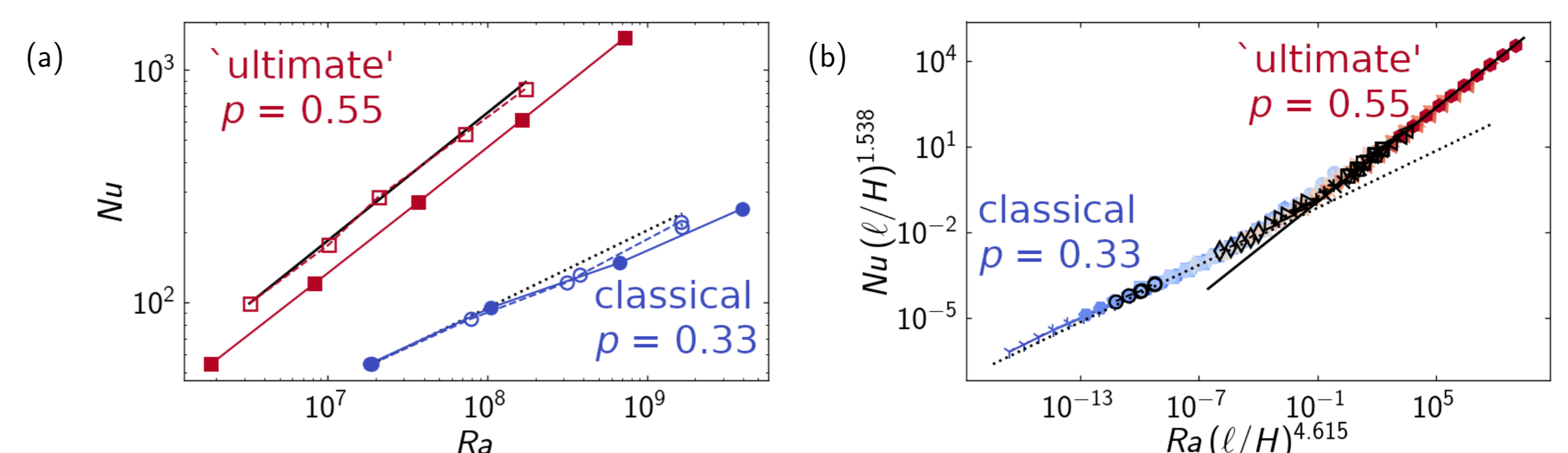


Figure 3: Scaling regimes of the heat transfer in radiatively driven turbulent thermal convection at  $Pr = 1$ . (a)  $Nu$  vs.  $Ra$  for  $\ell/H = 10^{-4}$  (classical) and  $\ell/H = 0.05$  ('ultimate') showing ODT (filled) and experiments [2] (open symbols). (b) Rescaled  $Nu/Nu_X$  vs.  $Ra/Ra_X$  for ODT covering  $10^{-5} \leq \ell/H \leq 0.4$  (blue-to-red symbols). Experiments (black symbols) are from [2, 3].

## Joint probability density of turbulent eddy size and location

ODT yields turbulence statistics as simulation result. Conditional **eddy event statistics** yield surrogate turbulence spectra by a built-in wavelet transformation due to the triplet-map (Fig. 1) formulation.

- **Fig. 4(a)** shows the **joint probability density function (jPDF)** of the log-scaled ODT eddy size  $\lambda$  and location  $z_0$  over the bottom wall for the **classical regime** with  $\ell/H = 3 \times 10^{-5}$ ,  $Ra_0 = 10^{13}$ ,  $Pr = 1$ . The **broad peak** at the bottom right is bulk turbulence. The **narrow band** on the lower left is small-scale wall-attached turbulence.
- **Fig. 4(b)** shows the corresponding jPDF for the **'ultimate' regime** ( $\ell/H = 0.096$ ) in which only bulk but **no wall-attached turbulence** can be discerned.

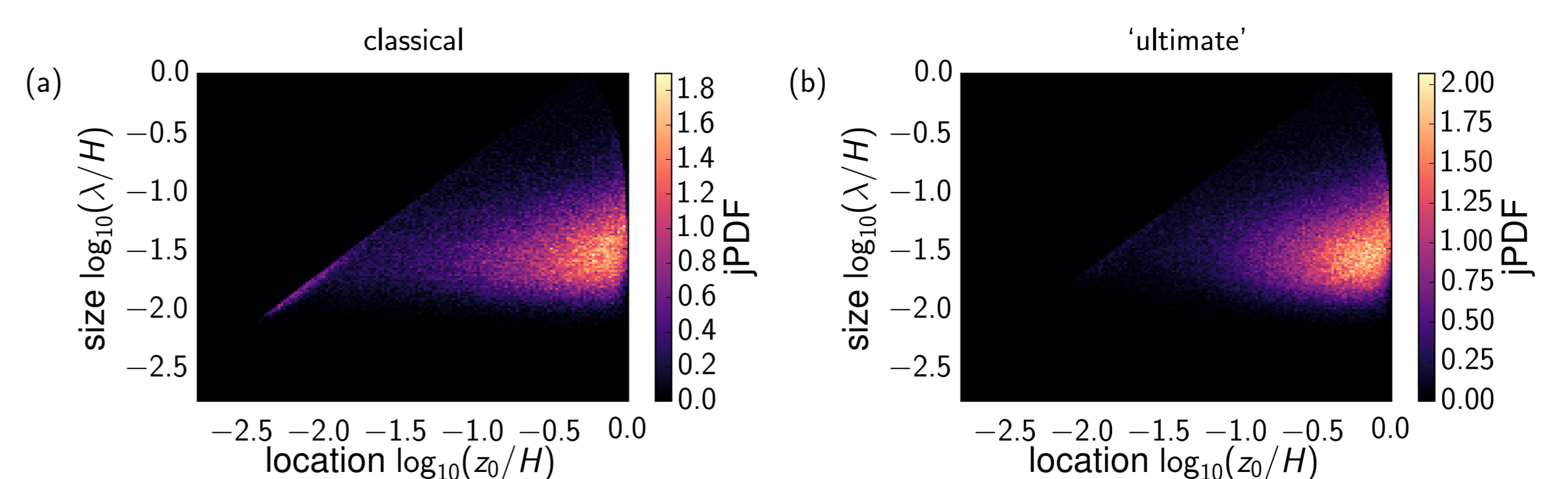


Figure 4: Joint probability density function (jPDF) of ODT eddy size  $\lambda$  and location  $z_0$  for  $Ra_0 = Ra Nu = 10^{13}$  and  $Pr = 1$ . (a) Classical regime for  $\ell/H = 3 \times 10^{-5}$ . (b) 'Ultimate' regime for  $\ell/H = 0.096$  lacks small wall-attached eddies.

## Conclusions

- ODT **reproduces and extrapolates** reference experiments [2, 3] with **fixed model parameters**.
- ODT predicts a **turbulent transition** from the classical ( $p \approx 0.33$ ) to the **'ultimate' regime** with scaling exponent  $p \approx 0.55$  consistent with reference measurements [2, 3].
- ODT results suggest **less small-scale wall-attached eddies** after transition to the **'ultimate' regime**. This is consistent with the transition in thermal convection between permeable walls [14].

## Forthcoming research

- Radial transport [15] and radial buoyancy in cylinders or spheres [16]
- Model application to Taylor–Couette flow with extension to angular momentum transport

## References

- [1] F. H. Busse, *Physics* **5**, 4 (2012).
- [2] S. Lepot, S. Aumaitre, B. Gallet, *PNAS* **115**, 8937 (2018).
- [3] V. Bouillaut, S. Lepot, S. Aumaitre, B. Gallet, *J. Fluid Mech.* **861**, R5 (2019).
- [4] L. R. M. Maas, *J. Fluid Mech.* **437**, 13–28 (2001).
- [5] A. Ghasemi, M. Klein, A. Will, U. Harlander, *J. Fluid Mech.* **853**, 111–149 (2018).
- [6] F. Chillà, J. Schumacher, *Eur. Phys. J. E* **35**, 58 (2012).
- [7] A. R. Kerstein, *J. Fluid Mech.* **392**, 277 (1999).
- [8] D. O. Lignell, A. R. Kerstein, G. Sun, E. I. Monson, *Theor. Comput. Fluid Dyn.* **27**, 273 (2013).
- [9] S. Wunsch, A. R. Kerstein, *J. Fluid Mech.* **528**, 173 (2005).
- [10] E. D. Gonzalez-Juez, A. R. Kerstein, D. O. Lignell, *Geophys. Astro. Fluid Dyn.* **107**, 506 (2013).
- [11] M. Klein, H. Schmidt, *Proc. 11th Int. Symp. Turb. Shear Flow Phen.* (Southampton, UK, 2019), vol. 1, pp. 1–6.
- [12] S. Grossmann, D. Lohse, *J. Fluid Mech.* **407**, 27 (2000).
- [13] W. V. R. Malkus, *Proc. Royal Soc. Lond. A* **225**, 185 (1954).
- [14] K. Kawano, S. Motoki, M. Shimizu, G. Kawahara, *J. Fluid Mech.* **914**, A13 (2021).
- [15] D. O. Lignell, et al., *Theor. Comput. Fluid Dyn.* **32**, 495 (2018).
- [16] M. Klein, H. Schmidt, D. O. Lignell, *Proc. Conf. Model. Fluid Flow (CMFF'18)*, J. Vad, ed. (Budapest, Hungary, 2018).